AD-759 125

WEAR AND EROSION CHARACTERISTICS OF A CAST COBALT BASE ALLOY

William T. Ebihara

Army Weapons Command
Rock Island, Illinois

January 1973

DISTRIBUTED BY:

NTIS

National Technical Information Service
U. S. DEPARTMENT OF COMMERCE
5285 Port Royal Road, Springfield Va. 22151

AD 751825

AD

SWERR-TR-73-2

WEAR AND EROSION CHARACTERISTICS OF A CAST COBALT BASE ALLOY

TECHNICAL REPORT

William T. Ebihara

D D C
REPRODUCED
APR 30 1973
RESULTS

January 1973

Reproduced by
NATIONAL TECHNICAL
INFORMATION SERVICE
U S Department of Commerce
Springfield VA 22151

RESEARCH DIRECTORATE
WEAPONS LABORATORY, WECOM
RESEARCH, DEVELOPMENT AND ENGINEERING DIRECTORATE
U. S. ARMY WEAPONS COMMAND

Approved for public release, distribution unlimited.

56

DISPOSITION INSTRUCTIONS:

Destroy this report when it is no longer needed. Do not return it to the originator.

DISCLAIMER:

The findings of this report are not to be construed as an official Department of the Army position unless so designated by other authorized documents.

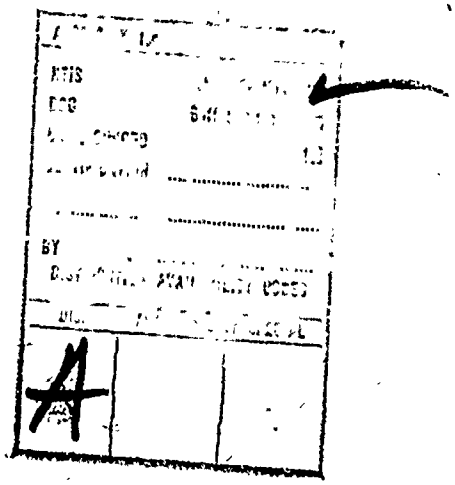

Unclassified

Security Classification

DOCUMENT CONTROL DATA - R & D

(Security classification of title, body of abstract and indexing annotation must be entered when the overall report is classified)

1. ORIGINATING ACTIVITY *(Corporate author)*
U. S. Army Weapons Command
Research, Dev. and Eng. Directorate
Rock Island, Illinois 61201

2a. REPORT SECURITY CLASSIFICATION
Unclassified

2b. GROUP

3. REPORT TITLE
WEAR AND EROSION CHARACTERISTICS OF A CAST COBALT BASE ALLOY (U)

4. DESCRIPTIVE NOTES *(Type of report and inclusive dates)*
Technical Report

Details of illustrations in this document may be better studied on microfiche.

5. AUTHOR(S) *(First name, middle initial, last name)*
William T. Ebihara

6. REPORT DATE	7a. TOTAL NO. OF PAGES	7b. NO. OF REFS
January 1973	54	14

8a. CONTRACT OR GRANT NO.	9a. ORIGINATOR'S REPORT NUMBER(S)
b. PROJECT NO. DA 1T061102B32A	SWERR-TR-73-2
c. AMS Code 501B.11.85500.01	9b. OTHER REPORT NO(S) *(Any other numbers that may be assigned this report)*
d.	

10. DISTRIBUTION STATEMENT
Approved for public release, distribution unlimited.

11. SUPPLEMENTARY NOTES	12. SPONSORING MILITARY ACTIVITY
	U. S. Army Weapons Command

13. ABSTRACT

(U) An investigation was conducted at the Research Directorate, Weapons Laboratory, USAWECOM, to determine the erosion and wear characteristics of a conventional-cast gun tube material, Haynes Stellite Alloy No. 21, (HS-21), and to relate mechanical properties and structural aspects of the alloy to these characteristics. A significant portion of this effort was applied to the construction and development of a special wear-test apparatus capable of variable load and sliding speed, ultra-high vacuum, gaseous environments, and elevated temperature testing. The room-temperature wear tests in vacuum were characterized by reduced friction coefficients as compared with oxide debris and increased wear track dimensions observed for HS-21 specimens tested in air. The morphology and distribution of carbides found in the cast structure appeared to be important factors for enhancing abrasive wear resistance. The as-cast specimens yielded superior wear resistance when compared with solution-treated and aged specimens of higher hardness. To supplement these wear tests, tensile, fatigue, thermal exposure and gas-particulate erosion tests were conducted in an effort to relate the properties of the material to the erosion behavior in actual gun tubes. Deformation rates appeared to be critical in evaluating mechanical properties of cast HS-21 especially under the conditions of rapid-fire weapons where high strain rates would tend to increase strength and ductility. Significant aging occurs above 1200°F for specimens tested at low strain rates which resulted in limited ductility for the alloy. (U) (Ebihara, William T.)

DD FORM 1 NOV 68 1473 REPLACES DD FORM 1473, 1 JAN 64, WHICH IS OBSOLETE FOR ARMY USE.

Unclassified

Security Classification

14. KEY WORDS	LINK A		LINK B		LINK C	
	ROLE	WT	ROLE	WT	ROLE	WT
1. Gun Tube Erosion						
2. Abrasive Wear						
3. Cobalt-Base Alloy						
4. Wear Tests						
5. Mechanical Properties						
6. Structural Stability						

AD

RESEARCH DIRECTORATE

WEAPONS LABORATORY, WECOM

RESEARCH, DEVELOPMENT AND ENGINEERING DIRECTORATE

U. S. ARMY WEAPONS COMMAND

TECHNICAL REPORT

SWERR-TR-73-2

WEAR AND EROSION CHARACTERISTICS OF A CAST COBALT BASE ALLOY

William T Ebihara

January 1973

DA 1T061102B32A AMS Code 501B.11.85500 02

Approved for public release, distribution unlimited.

CONTENTS

Preceding page blank

TABULAR DATA

ILLUSTRATIONS

ILLUSTRATIONS (continued)

ACKNOWLEDGMENTS

The author wishes to acknowledge the advice of Dr. Donald H. Buckley of the NASA-Lewis Research Center on wear test techniques and equipment, the assistance of Mr. Robert D. Busch in the construction and development of the wear test apparatus, and the participation of Mr. William V. Cassell for the conducting of tensile and fatigue tests.

INTRODUCTION

Gun tube erosion remains an extremely serious problem that results in large monetary expenditures and a safety hazard to operating personnel. Because of the complex nature of gun tube erosion and the attendant lack of understanding, with respect to it, erosion control methods, in the past, were based on empirical trial-and-error techniques. Although considerable improvements in weapon performance have been made (e.g., improved platings, liners, propellants, wear-reducing additives), large gains in erosion reduction are still limited by the lack of fundamental knowledge concerning erosion mechanisms or the erosion rate, i e , controlling parameters for any given weapons system

One major element necessary to describe erosion is that of the behavior of the gun tube material in its response to the repetitive thermal - chemical - mechanical loading conditions of firing Therefore, in an effort to accumulate fundamental knowledge of gun tube erosion, a study was undertaken at the Research Directorate, Weapons Laboratory, USAWECOM, to examine the erosion and wear characteristics of a common gun tube liner material, Haynes Stellite Alloy No 21, (HS-21) and an attempt made to relate these characteristics to the properties of the material.

As is the case for several ordnance materials currently used for elevated temperature service, the origin of HS-21, a cast cobalt-alloy used as gun tube insert liner material, lies in aircraft application. A great demand existed in the late thirties for thermal-resistant materials for use in aircraft turbo chargers - A denture alloy, Vitallium, with an original composition of 27 w/o Cr, 5 w/o Mo, 0 5 w/o C, the balance being Co, was modified with a reduced carbon content, (0 3 w/o C), for aircraft engine application.[2] However, excessive age hardening persisted, even with the reduced carbon level and caused further modification of a 2.5 w/o Ni addition to inhibit this tendency. This alloy was designated HS-21 or modified Vitallium.

Then, with this country's involvement in World War II, military requirements, especially for aerial combat situations, pressed urgent demands for hot-hard gun tube materials for use in rapid-fire machine guns By the fall of 1942, efforts were focused on the preparation of chromium and molybdenum in a form suitable for use as gun liners.[3] Further efforts of this phase, in 1943, resulted in the cobalt - chromium alloys, referred as Stellites. By 1945,

based on the results of successful test firings, production of the HS-21 insert-lined caliber .50 machine gun barrels was initiated. Although several materials were evaluated, none were as successful as HS-21 as an insert liner material.

Vent plug and test firings were also conducted on pure cobalt. When a short, rifle, caliber .30, liner of pure swaged cobalt was test fired, it exhibited resistance to powder-gas erosion but possessed insufficient hot-hardness to resist rifling deformation caused by the projectiles.[4] Efforts were then made to harden cobalt and to possibly increase gas erosion resistance by addition of varying amounts of tungsten, molybdenum, or chromium. One of these alloys containing 93 per cent cobalt and 7 per cent tungsten performed very well when tested as a liner in the caliber .50 machine gun.[5] However, no further development of these alloys as liners was pursued for the following reasons: (1) these alloys had a high content of the then critical metal cobalt, (2) these alloys were difficult to process compared with investment casting of HS-21, and (3) no marked test firing performance advantage was evident over HS-21.

Firing tests[6] with the caliber .50 machine gun were made with other Stellite-type alloys to compare the performance of the alloys with the HS-21 performance and to see if alloys containing less cobalt (which was then in short supply) could be substituted for HS-21. Tungsten-bearing Stellite alloys, listed in Table I, were tested. All were inferior with respect to performance when compared with HS-21, and greater land wear was observed. Deep cracks were also revealed for all the alloys with the exception of Alloy No. 23; brittle failure resulted during the firing test. Two molybdenum containing Stellite alloys in which nickel had been added were also tested as liners. Stellite 422-19 showed excessive land wear. The investment-cast liner of Stellite 27 initially exhibited performance equal to HS-21; however, on subsequent testing, complete land wear was observed after a 300-round burst.

The Stellite insert liner concept was then adapted to the caliber .30 machine gun and later to the caliber .60 weapon which was ready for production by the end of the war. Further application of Stellite (HS-21) and other hot-hard alloys to small arms barrels was continued by the Crane Company after the war. Because of the limitations of the HS-21 to be thermally resistant in hypervelocity conditions with double-base propellant, attempts were made to protect the Stellite bore surface with higher melting point platings. However, electroplated chromium exhibited poor adherence, and pyrolytic molybdenum coatings were unsatisfactory because of the formation of a brittle intermetallic compound during firing.

TABLE I

NOMINAL COMPOSITION OF STELLITE ALLOYS
(COMPOSITION IN WEIGHT PER CENT)

Alloy (No.)	Cr	Ni	W	Mo	C	Co
21	27	2	-	6	0.25	64
6	28	2	5	-	0.50	64
23	25	2	5	-	0.40	67
X-40	25	10	7	-	0.50	57
422-19	25	16	-	6	0.40	52
27	28	32	-	5	0.40	34

A parallel effort led to the development of nitrided, chromium-plated, caliber 50 gun barrels. Eventually, improvements to the Stellite-inserted barrel were made by use of a chromium-plated steel bore ahead of the Stellite liner and constriction of the bore at the muzzle

Although a general description of the physical metallurgy of HS-21 was presented in the earlier report, it is worthwhile to present the basic characteristics of the alloy again. The alloy is hardened by carbide formation and, to a lesser degree, by solid-solution strengthening. Chromium and molybdenum are the carbide forming elements as well as the solid solution hardeners. The carbides found in the cast HS-21 include M_7C_3, $M_{23}C_6$, M_6C, and Cr_3C_2. The stability of the carbides depends on both the temperature and the carbide composition relative to that of the matrix. The chromium additives provide hot-corrosion and oxidation resistance, whereas nickel tends to stabilize the α-matrix or fcc structure

The normal matrix phase for HS-21 is generally face centered cubic because the $\alpha(fcc) \rightarrow \varepsilon(hcp)$ is generally quite sluggish from room temperature to 800°C. The stacking fault energy is quite low in these types of alloy; this condition results in a very low M_s temperature (below RT) for the

martensitic-type $\alpha \rightarrow \varepsilon$ transformation.[8] Mechanical deformation at room temperature may bring about this transformation, however.

The results of the initial study to describe the characteristics of the cast cobalt-alloy after being subjected to actual test firing conditions were reported earlier.[1] In this current effort, the special wear test apparatus, the room temperature wear test results, and the properties relevant to the wear-resistant character of HS-21 are described

EXPERIMENTAL PROCEDURE

Materials

All test specimens used for mechanical testing purposes were taken from cast HS-21 rods. The fatigue and tensile test specimen axis coincided with the longitudinal axis of the cast rods. Wear test disk specimens were obtained by the sectioning of cast rods so that the wear surface would be perpendicular to the rod axis. The chemical analysis for the rod material obtained from Cabot Corporation is as follows:

	Cr	Fe	C	Si	Co	Ni	Mn	Mo
Weight %	27.06	1.71	0.29	0.54	bal.	2.48	0.65	5.84

The hemispherical rider material consisted of 91% WC - 9% Co (designated as 9H C2).

Wear Test Apparatus

The test device used in this investigation is a pin-on-disk wear tester as shown in Figures 1 and 2. This apparatus was constructed from a basic design provided by NASA Lewis Research Center.[9] The specimen (A in Figure 1) consisted of a 4-cm-diameter HS-21 disk, and the rider was a 0.950-cm-diameter hemispherical tungsten carbide rod (B). The disk was mounted on a shaft magnetically driven by a motor and gear assembly (C in Figure 2). Although such a drive assembly allows for variable speed, a linear sliding velocity of approximately 2 cm/sec was used in most of the tests. All wear tests were multiple-pass runs -- 1000 total cycles.

The carbide rider was positioned on a gimble-mounted arm (D), vacuum-sealed by means of a bellows assembly. The

rider was dead-weight-loaded against the disk surface by a pulley assembly (E) attached to the arm. A strain gage system (F) was positioned perpendicular to the loading direction, and the frictional force was monitored continuously on a sensitive chart recorder (G). In most of the tests, an applied load of 400 grams was used which resulted in a Herzian contact pressure of 93,000 psi

After the specimen was placed in the chamber and the chamber flange (H) closed, the system was rough-pumped to approximately 1 Torr by means of a cryogenic sorption pump (I). Further evacuation was achieved by a titanium sublimation pump (J) and an ion pump (K) which reduced the pressure to approximately 10^{-9} Torr. The motor-drive mechanism was then activated and the weights (E) were added to the loading device to start the wear test The frictional force was monitored and recorded throughout the test and wear track measurements and metallographic evaluations were made after testing For elevated temperature testing purposes, an electron gun heating source was provided The electron gun control assembly (L) and the filament transformer housing (M) are shown in Figure 2.

Prior to the construction of the ultrahigh vacuum wear tester, tests involving HS-21 specimens were conducted on a Falex (Faville-LeValley) lubricant test machine. This apparatus comprises a rotating ¼-inch-diameter pin clamped between two V-shaped blocks in a nutcracker-type arrangement so that the load can be applied to the pin through the blocks. With increasing load, line contact shifts to load area contact, and wear can be measured by determination of the wear track width or the weight loss of the pin and blocks. Although this device is generally utilized to test lubricants, no external lubrication was used in this study The operating speed was 290 rpm and the specimens were weighed before and following the wear test on analytical balances sensitive to within ± 0 1 mg

The pin material consisted of chromium-plated SAE 3135 steel, although one test was conducted with a 90-10 cartridge brass pin. The block specimens consisted of HS-21 in the as-cast, solution-annealed, and annealed-and-aged conditions. The average Rockwell-C hardness values for the block specimens were 28 8, 29 7 and 39.1, respectively.

Mechanical Testing

Tensile test specimens were made from 3/8-inch-diameter cast rods of HS-21 The configurational and dimensional details of the specimen are shown in Figure 3 The specimens

were tested in 10^{-5} Torr vacuum at elevated temperatures with an Instron machine. Nominal soak time at the test temperature before testing was 20 minutes. The test temperatures ranged from room to 1700°F Strain rates of 0.005 and 0.5 min^{-1} were used in the tests

Fatigue test specimens were also machined from 3/8-inch diameter cast rods to the configuration shown in Figure 4. The specimens were loaded unidirectionally in the Sonntagg test unit with load cycles varying from zero to a maximum tensile load All tests were conducted in air at room temperature with a load application frequency of 1800 cpm.

Structural Stability Tests

Test specimens were sectioned from one-inch-diameter, 3/16-inch-thick, cast HS-21 disks. The first series of tests were conducted to ascertain the transient liquation range of the as-cast HS-21 alloy. A ten-minute dwell time at the test temperature was used, followed by rapid quenching in oil. The samples were then mounted in epoxy and prepared for metallographic examination

Tests were also conducted on HS-21 to determine the structural stability of the matrix under thermal and mechanical loading conditions Mechanically cut chips of the cast alloy were collected and analyzed by X-ray diffraction techniques. Long-term thermal exposure tests were also conducted to determine the phase stability characteristics of the alloy

RESULTS AND DISCUSSION

Gun tube erosion remains an unresolved complex phenomenon due primarily to the nature of the multivariant response of the material to thermal-chemical-mechanical loading of actual firing conditions In small caliber rapid-fire weapons, much of the material damage occurs in the form of granular or particulate attrition from the bore surface region as opposed to thermal melting or ablation as found in large caliber gun tubes Therefore, the wear phenomenon in small caliber gun tubes should be related to energy-absorbing characteristics under repetitive loading conditions and reactive environments. In the past, hardness was generally considered to be a characteristic material parameter in ascribing anticipated wear resistance However, depending on the loading conditions and the materials in contact, other material properties such as yield strength, fracture toughness, work-hardening, and fatigue resistance may more adequately relate to the wear-resistance character of the material

Test-Fired 7.62mm HS-21 Inserts

The earlier publication reported the microstructural changes observed in the cast HS-21 structure when subjected to actual test firings. Since that reporting period, topographical studies were made with a scanning electron microscope A scanning electronmicrograph of the land-groove area of a 7.62mm HS-21 M60 insert in the as-machined condition is shown in Figure 5. Note that the land surface appears much rougher than the adjacent groove surface. After one round of fire, the interior bore surface became caked with the propellant debris (Figure 6) The surface striations were observed to be less prominant on the rifling surface compared with the as-machined condition. A surface crack is noted in the same figure at the land-groove corner.

After 100 rounds, the corners of the rifling became rounded and the transverse surface cracking was intensified The land surface became much smoother and widespread layering of the propellant debris was noted (Figure 7) After 3000 rounds, the surface cracks appeared quite pronounced (Figure 8a) and debris was extruded into the crack openings (Figure 8b) No evidence of the original roughened surface or striations on the land was noted, and the density of cracks appeared much higher for the land surface compared with the groove region.

Examination of a 7 62mm insert after more than 28,000 rounds showed extensive surface cracking and further rounding of the rifling corners (Figure 9a). A longitudinal section of the insert is shown in an optical photomicrograph (Figure 9b) of the depth of the surface cracks Cracking was also observed to extend to the groove region, and large cavities were noted (Figure 10)

The previous work indicated evidence primarily for gross material removal in 7.62mm HS-21 inserts caused by the intersection of cracks that propagated either along the grain boundary carbides or on principal slip planes The current study has shown that surface material removal can occur in finite regions without the necessity of cracking along grain boundary carbides

Silica Grit Erosion Tests

The topographic observations on test-fired HS-21 inserts led to a cursory investigation of the resistance of the material to erosion in a gas-particulate jet stream. Tests in a Vacu Blast Model B apparatus were performed with the jet

impingement angle parallel and normal to the bore surface. The gas velocity was calculated to be approximately 780 ft/sec at the orifice and the total test time was five minutes in each case. The silica particle size distribution is typified in Figure 11.

Gas-particle jet streams parallel to the bore axis did not appreciably erode the HS-21 specimen as shown in Figure 12a. Upon closer inspection of the groove area, Figure 12b, surface material flow was evidenced. The sample exposed to the jet stream, normal to the bore surface, became extensively eroded, as shown in Figure 13a. In this case, the land and groove areas were equally eroded, and carbide islands were shown to remain (Figure 13b).

The cast HS-21 behaves much like that of the brittle material in Bitter's model for deformation wear.[9] In his model, deformation wear is associated with repeated blows by particles impacting normally against the material surface, and which eventually cause cracking and spalling of the surface material. However, the actual internal ballistics conditions in gun tubes more closely resemble that of abrasive erosion or cutting wear phenomenon. In this case, the particles act as a cutting edge of a tool which moves into the specimen surface, and cause plastic deformation and removal of the formed debris. Finnie[10] constructed an analytical model for such a wear mode, and correlation was found for ductile specimens at small angles of attack. Nelson and Gilchrist[11] further elaborated on the distinction between the cutting wear and the deformation wear factors. The wear factor is associated with the micromachining action of abrasive particles which attack the surface under a small angle. The deformation factor is associated with impingement erosion or impact under approximately 90 degrees. The Nelson and Gilchrist model for erosive wear is given in the Appendix.

Tensile Tests

The tensile test data of the as-cast HS-21 material are tabulated in Table II. Yield strengths, ultimate tensile strengths and elongation values are shown graphically in Figure 14 for tests conducted at 0.005 and 0.5 min^{-1} strain rates. The yield strength for both strain rates was observed to decrease with temperature up to 1400°F and then increase at 1500°F, falling off again at 1700°F. The observed yield strength increase is thought to arise because of the increased rate of strain-assisted second phase precipitation which offsets the rate of recovery at 1400°F. These precipitates would also contribute to increased dislocation pileups. Corresponding increases in ultimate tensile strengths above 1400°F are not observed because of the decreased ductility.

TABLE II

TENSILE TEST RESULTS FOR CAST HS-21 BARS

	Test Temperatures					
	RT	1200°F	1400°F	1500°F	1600°F	1700°F
0.005 min^{-1}						
0.2% Yield Strength (ksi)	72.5	49.9	40.8	52.3	50.0	29.0
Ultimate Strength (ksi)	106.0	87.3	64.9	55.0	53.0	31.4
Elongation (%)	14.5	16.5	13.0	4.0	1.0	1.5
0.5 min^{-1}						
0.2% Yield Strength (ksi)	80.0	47.2	41.5	59.0	52.2	42.5
Ultimate Strength (ksi)	116.0	106.0	89.0	67.2	61.2	61.2
Elongation (%)	17.0	27.0	25.0	3.0	4.0	12.0

Note, in Figure 14, that the elongation values undergo a minimum around 1500° to 1600°F. The ultimate tensile strength was increased with the higher strain rate. This observation is attributed to the work-hardening characteristics of HS-21 at the lower temperatures. The amount of strain-aging was reduced at elevated temperatures with the higher strain rate, and, greater ductility was observed. A typical example of the load-extension curves for cast HS-21 tested at two different strain rates is graphically shown in Figure 15.

Fatigue Tests

The results of the room temperature fatigue tests on cast HS-21 are presented in Figure 16 in the form of an S-N plot While these results do not appear particularly relevant to actual gun tube loading and temperature conditions, they can be used as a reference basis for analyzing erosion or fracture damage Although the room temperature fatigue resistance appears adequate for gun tube service, significantly lower fatigue limits are expected at elevated temperatures. Generally, the effect of temperature is to shift the S-N curve parallel to the stress axis without significantly altering the mean value of the slope. Therefore, with yield strength as a reference in the S-N plot, the 1200°F to 1400°F temperature range becomes critical for cast HS-21 inserts if the resultant tensile stress is assumed to be due entirely to the pressure pulse (50 ksi for WC846 propellant used in 7 62mm ammunition) for the M60 weapon. However, such predictions are not warranted at this time due to the undefined nature of other factors as thermal, shrinkfit, and residual stresses as well as high strain-rate conditions in rapid-fire gun tubes

Thermal and Structural Stability Tests

The as-cast structure of HS-21 is shown in Figure 17. Numerous small, well-distributed areas of eutectic carbides can be observed. The binary eutectic is the M_6C type and the ternary form includes the M_6C, the Cr_7C_3, and-or the $M_{23}C_6$ phases (M represents any carbide forming element). Carbides are also observed to line the grain boundaries. Upon heating to temperatures above 2200°F, the carbides dissolved into the matrix Note the decreased carbide size in the sample held for 10 minutes at 2240°F (Figure 18), however, the 2280°F exposure caused liquation in the carbide zones as observed in Figure 19. Further liquation can be seen in Figure 20, where the specimen was heated to 2310°F.

A variation in the melting range is expected in these multi-component alloys; however, the observed transient melting temperature of 2280°F is considerably lower than the reported 2465°F temperature [3].

Since the hcp phase is the equilibrium room temperature structure for the HS-21 alloy matrix, thermal exposure runs were performed on specimens to test the stability of the fcc matrix. X-ray diffraction techniques were used to detect the fcc and hcp structures. Because the cast HS-21 specimens contained large grains, sufficient diffraction lines could not be detected for meaningful measurement. Therefore, a fine-grained solution-annealed HS-21 specimen was used in the tests. As shown in Figure 21, the X-ray pattern reveals the fcc (α) structure's diffraction lines for the solution-treated structure. After a 90-hour treatment at 1500°F, a significant portion of the specimen was transformed to the hexagonal phase (ε) as shown in Figure 21. The corresponding solution-annealed and striated structures are shown in an optical photomicrograph in Figure 22a and 22b. Considerable aging or carbide precipitation was noted in the striations. The striated structures were similar to those observed in the elevated temperature tensile test specimens. Similar striations, but without the excessive precipitation, were also noted near the bore surface of test-fired HS-21 inserts. Evidence for the extensive hcp transformation from the fcc matrix was shown on X-ray diffraction patterns of machined HS-21 chips. These results revealed that the matrix phase can easily transform to hcp platelets upon plastic deformation but that the thermal transition is sluggish and requires long-term exposure at elevated temperatures.

Falex Wear Tests

The test results of the Falex wear tests are given in Table III, in which the average weight change is shown for the pin and block specimens after testing. As observed in Figure 23 and the tabular results, very little adhesive wear was evidenced on HS-21 block specimens when loaded against the brass pin. However, a quantity of brass was transferred to the block specimens. When the Stellite blocks were in contact with the chromium-plated steel pins, the cobalt alloy was observed to wear preferentially. In the tests involving Cr-plated steel pins, HS-21 specimens were presented in three conditions: as-cast, solution-annealed, and solution-annealed plus an aging treatment. The hardness values of the as-cast and solution-annealed specimens were comparable; measurements ranged around R_C 28-30. The aged HS-21 specimen was considerably harder, exhibiting a value of R_C 39.

TABLE III

FALEX WEAR TEST RESULTS

Specimen Designation	Block Material	Weight Change (g)	Pin Material	Weight Change (g)
C 1A,B	as-cast 21	+0.0019	90-10 brass	-0.0050
C 2A,B	as-cast 21	-0.0054	Cr-plated steel	-0.0002
S 1A,B	SA*	-0.0085	Cr-plated steel	-0.0004
SA 2A,B	SA + age@	-0.0068	Cr-plated steel	-0.0004

* cast plus 2 hours at 2150°F

@ cast plus 2 hours at 2150°F plus 50 hours at 1350°F

The test results showed that the solution-annealed condition was most susceptible to abrasive wear; the as-cast sample exhibited slightly better wear resistance than the aged specimen.

The microstructures of the solution-annealed and aged specimens are exhibited in Figures 24a and 24b The solution-annealed specimen is not void of carbides but the coalescence of the primary carbides was observed (Figure 24a) The specimen which was solution-annealed and subsequently aged for 50 hours at 1350°F exhibited extensive carbide precipitation primarily on slip lines (Figure 24b) Although this type of structure is apt to enhance strengthening by the impedance of dislocation motion as reflected in the increased hardness value, crack propagation is also anticipated to proceed with ease by the branching out from larger carbides The wear resistance exhibited by the as-cast specimen was thought to be attributed to the presence of the large, blocky carbides and not primarily due to the average hardness of the alloy

Pin-on-Disk Wear Tests

The average friction coefficients and wear scar dimensions for the HS-21 specimens tested in air and in vacuum are presented in Table IV A plot of frictional force versus the number of cyclic passes for the specimens tested in air and in 10^{-3} Torr vacuum is shown in Figure 25 The enhanced friction observed for the specimen tested in air was attributed to the formation of debris (Figure 26a) Although the debris was not identified, it was believed to be cobaltous oxide The backscatter mode of radiation revealed that the debris consisted of lower atomic numbered elements (Figure 26b)

Unlike other wear systems such as iron or steel where the formation of an oxide film acts as a lubricant and reduces friction, the formation of cobalt oxide tended to increase friction as well as the wear track width In all probability, instead of forming a continuous stable oxide film, the cobalt oxide fragmented and acted as an abrasive, plowing into the alloy matrix and abrading the material. In a hard vacuum-environment where oxide formation was prevented, the rider plastically deformed the HS-21 alloy surface locally (Figure 27) Further penetration of the rider was prevented by the presence of the large surface carbides and the work-hardened surface layers The damage to the disk sample appeared quite localized Electrolytic etching with 2 per cent chromic acid did not reveal plastically deformed regions adjacent to the wear track

TABLE IV

PIN-ON-DISK WEAR TEST RESULTS

Test No.	Load (g)	Environment	Friction Coefficient	Scar Width (mils)	Scar Depth (mils)	Test Speed (RPM)	Surface Condition
4	387	760 Torr	0.68	10.6	0.079	11	as-machined
5	300	760 Torr	0.79	15.0	0.067	11	as-machined
7	400	760 Torr	0.84	15.0	0.142	11	as-machined
8	400	9×10^{-9} Torr	0.40	6.7	0.161	11	as-machined
9	400	9×10^{-9} Torr	0.45	13.0	0.185	11	0.05 micron*
10	400	7×10^{-9} Torr	0.45	10.1	0.051	44	0.05 micron*

*specimen polished with 0.05 micron abrasive

As shown in the plot (Figure 25) for the test conducted in air, friction increased continuously until approximately 200 passes when a quasi-steady-state condition was established. However, even during this steady state period, the frictional force varied considerably within a given pass due to the nonuniform debris formation in the wear track. The variation in frictional force in the 10^{-9} Torr vacuum test was lower than the 760 Torr test A typical frictional force-distance trace during one pass is shown in Figure 28.

No differences in friction or wear characteristics could be detected between an 8μ-in rms finish sample (test 8) and a 0.05μ-alumina grit-polished specimen (test 9). As shown in the tabular results, no significant differences in friction and wear characteristics can be attributed to the differences in surface roughness. Further, when the sliding speed was increased from the standard 2.0 cm/sec (11 rpm) for test 9 to 8.0 cm/sec (44 rpm) on test 10, the average coefficient of friction remained essentially the same for both cases Also, no significant differences in the wear scar characteristics could be observed

The vacuum wear tests were also characterized by evidence of transferred disk material on the rider tip (Figure 29a). The backscattered radiation photograph (Figure 29b) indicated that the attached material is of a lower atomic number than tungsten The X-ray distribution maps in Figure 29c and 29d show the characteristic radiation for cobalt ($K\alpha$) and tungsten ($L\alpha$), respectively This showed that the transferred material was rich in cobalt and, presumably, from the disk specimen

SUMMARY AND CONCLUSIONS

This effort concludes the study to evaluate erosion and wear characteristics of the cobalt alloy, HS-21 The characterization of structural damage to HS-21 liners is contained in the previous report In the present effort, a considerable portion of the work was applied to the development and construction of a special pin-on-disk wear test apparatus capable of variable loading and test speed, ultrahigh vacuum as well as controlled gaseous environments, and elevated temperature testing. The ultrahigh vacuum wear tests on cast HS-21 specimens yielded the following characteristics: (1) lower coefficient of friction compared with tests conducted in air, (2) no evidence of contamination in the wear track, (3) shallow and smoothly deformed wear tracks and (4) transferrence of disk material to the stylus The

presence of large, well-distributed carbides in the cast structure prevented significant penetration of the tungsten carbide stylus. The wear-resistance character of such carbides was also exemplified in Falex wear tests where HS-21 specimens of three different structural modifications were evaluated. In these tests, the as-cast specimens exhibited superior wear resistance compared with solution-treated and aged specimens of higher hardness. Further, the cast specimens showed excellent resistance to cutting wear in silica grit erosion tests where the jet flow was parallel to the specimen surface. At an impingement angle normal to the surface, however, the HS-21 matrix material was easily eroded away leaving numerous carbide islands.

In an attempt to relate certain material properties to the response of HS-21 to rapid fire conditions in small arms weapons, tensile, fatigue and structural stability tests were conducted. Transient liquation was observed to occur in the cast specimens at temperatures as low as 2280°F, which would limit the use of the alloy in hypervelocity weapons Increased ductility and strength with increased strain rate were observed for the cast alloy at elevated temperatures of interest in rapid fire weapons. These characteristics would tend to extend present material performance predictions which are based on standard low strain rate properties.

RECOMMENDATIONS FOR FUTURE WORK

Future efforts to evaluate materials performance in wear conditions found in rapid-fire gun tubes should be focused on areas of abrasive wear and impact-fatigue testing at elevated temperatures under controlled environments Attempts should also be made to quantify the wear behavior in terms of relevant physical properties and structural characteristics of the materials tested Further, analytical treatment of the laboratory test data as well as gun tube erosion test results should be attempted to arrive at predictive models that can be translatable to engineering design applications.

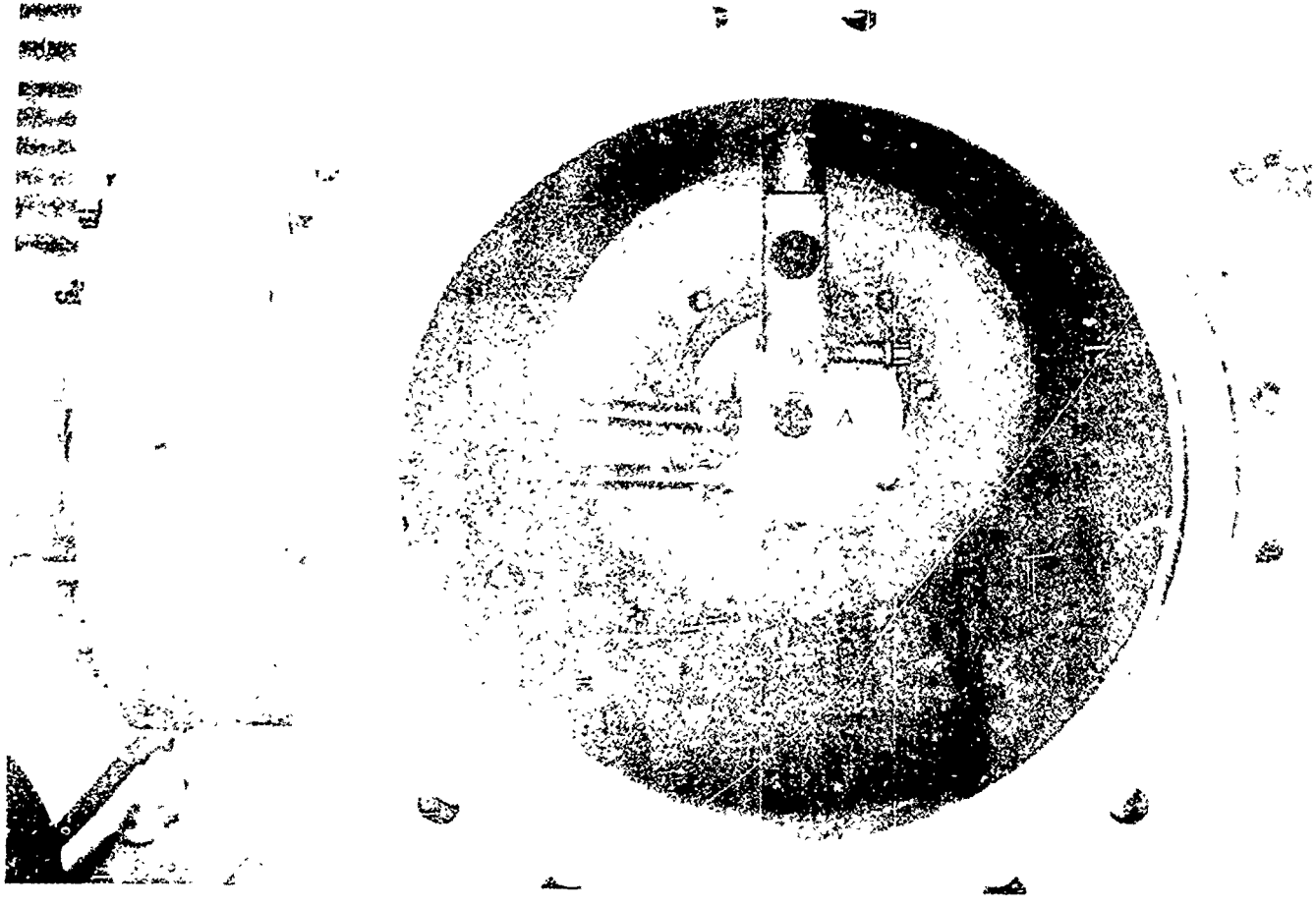

FIGURE 1 Wear Apparatus Chamber

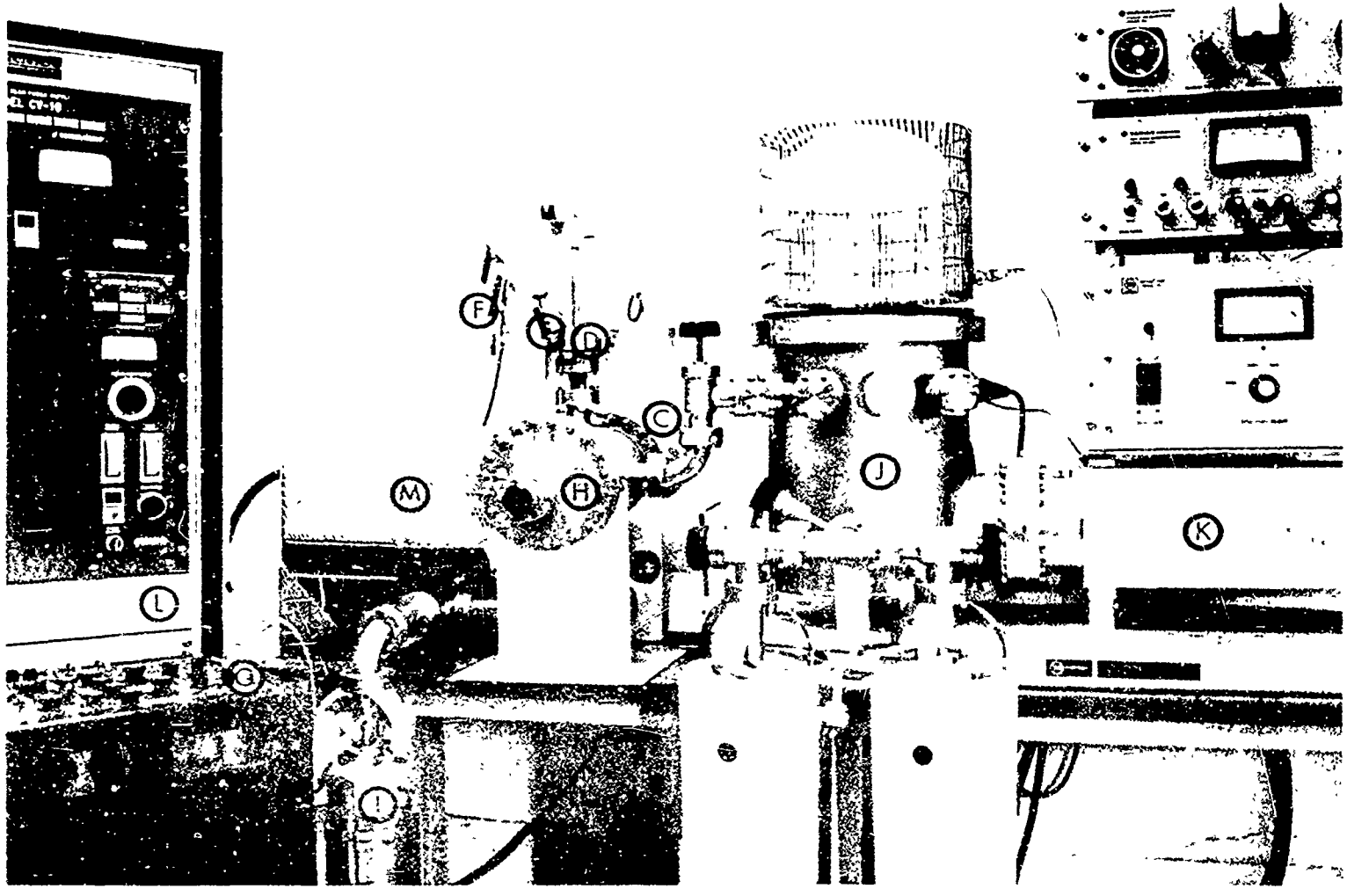

FIGURE 2 Wear Test Apparatus with Vacuum System

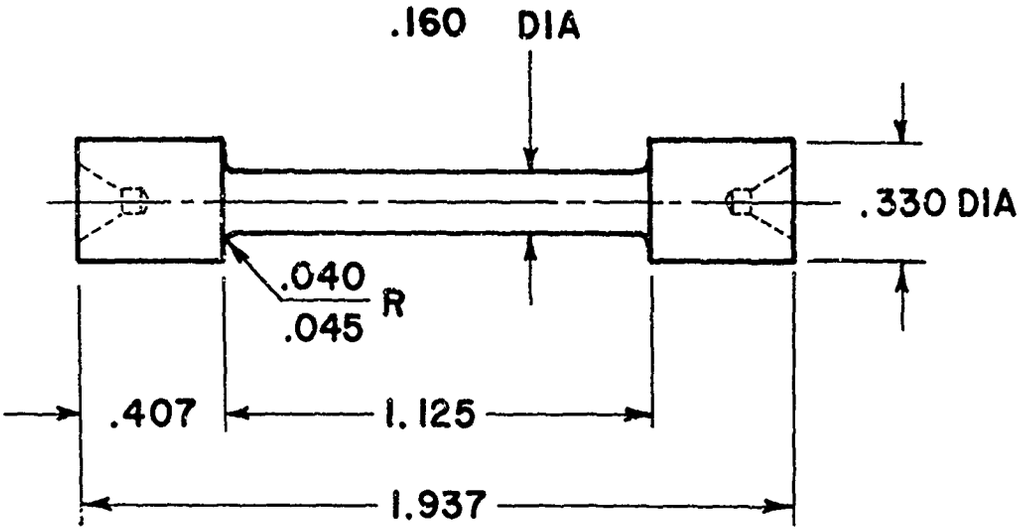

FIGURE 3 Tensile Test Specimen Configuration

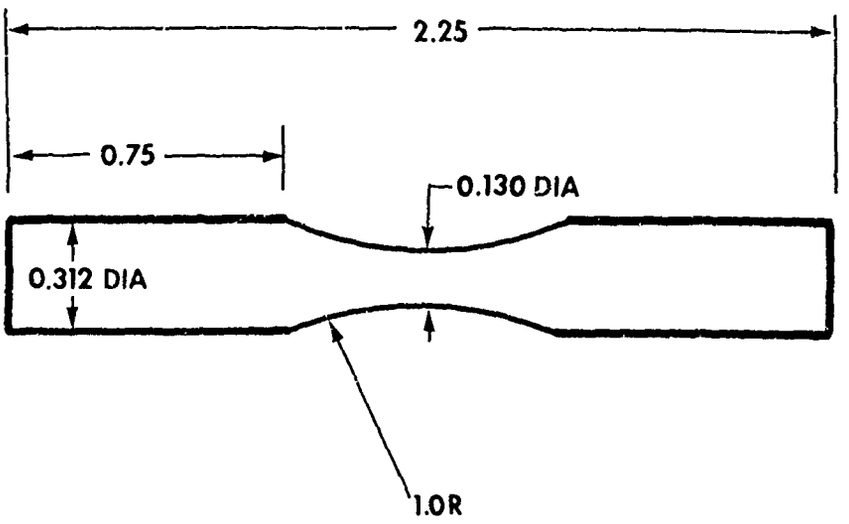

FIGURE 4 Fatigue Test Specimen Configuration

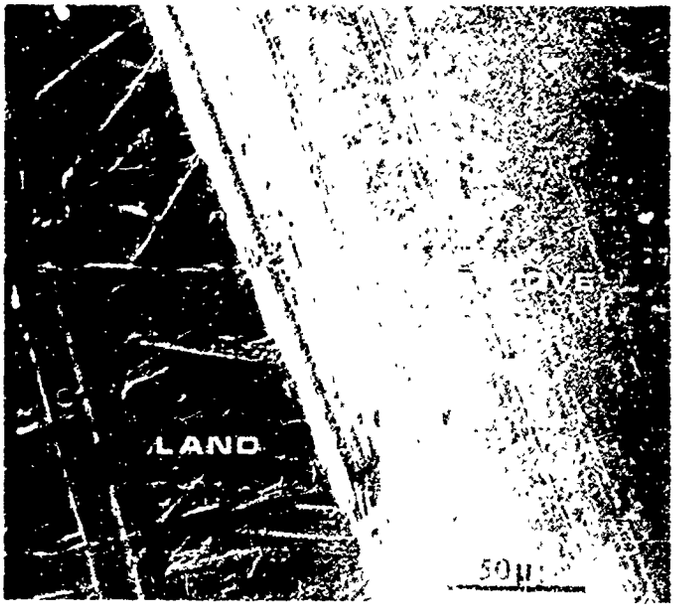

FIGURE 5 Scanning Electron (SEM) Micrograph of As-Machined Bore Surface

FIGURE 6 SEM Photograph of Bore Surface after One Round

FIGURE 7 Bore Surface after 100 Rounds (SEM)

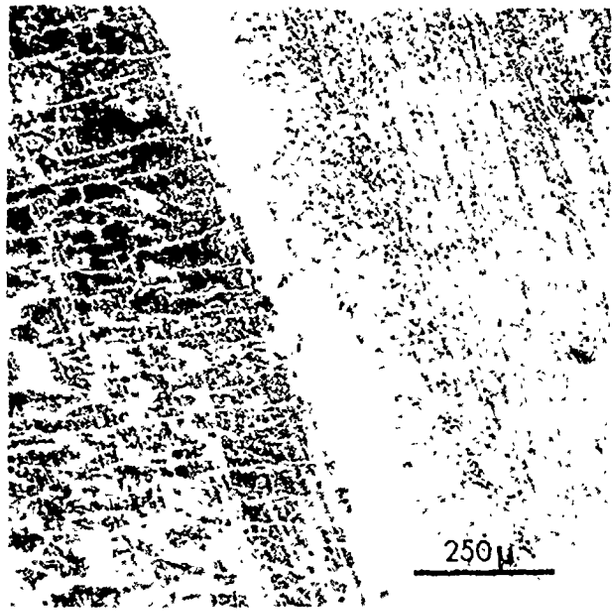

a

b

FIGURE 8 Bore Surface after 3000 Rounds (SEM)

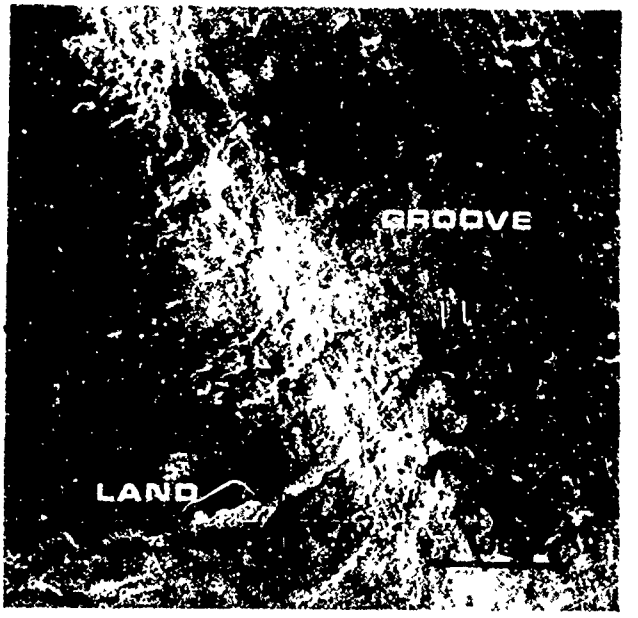

a. SEM Photograph

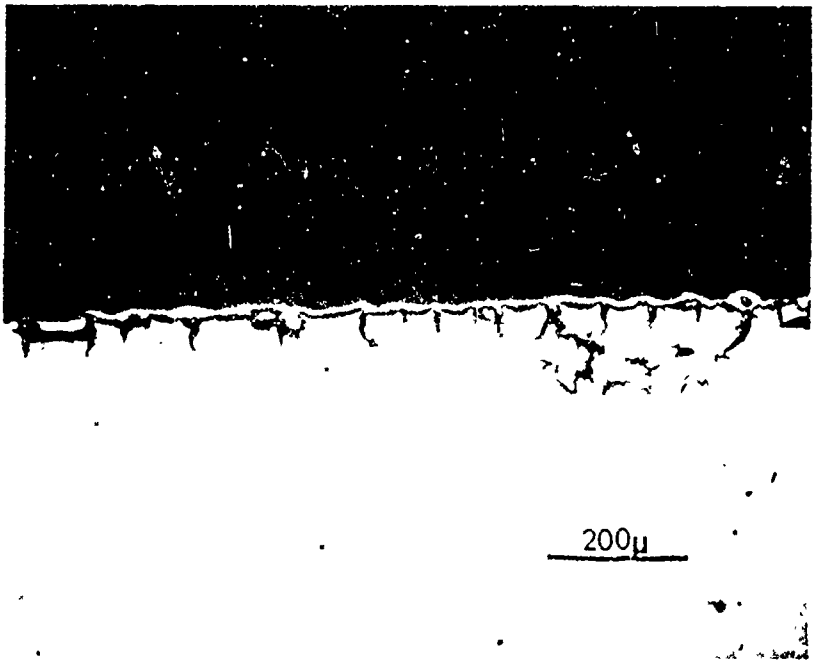

b. Optical Photomicrograph

FIGURE 9 Structure of Bore Surface Area after 28,410 Rounds

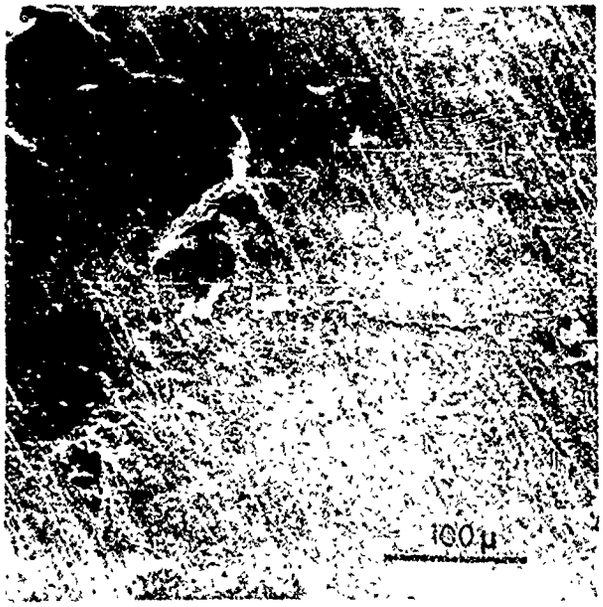

FIGURE 10 Surface Structure after 28,410 Rounds (SEM)

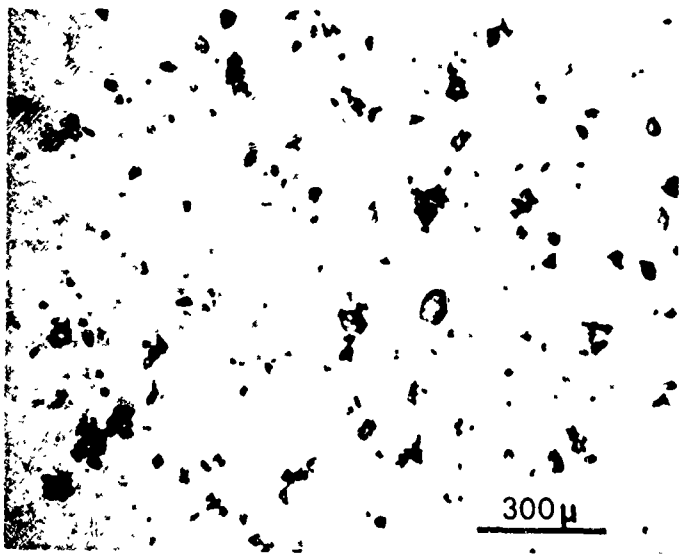

FIGURE 11 Optical Photomicrograph of Silica Particles used in Grit Blast Tests

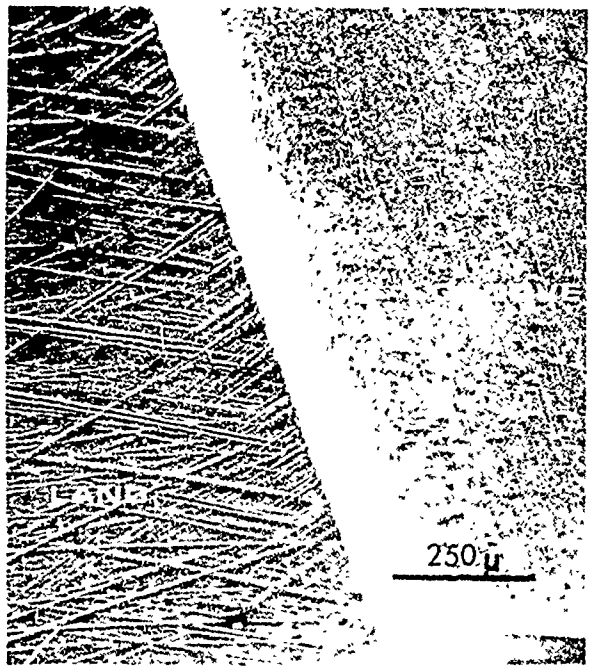

a

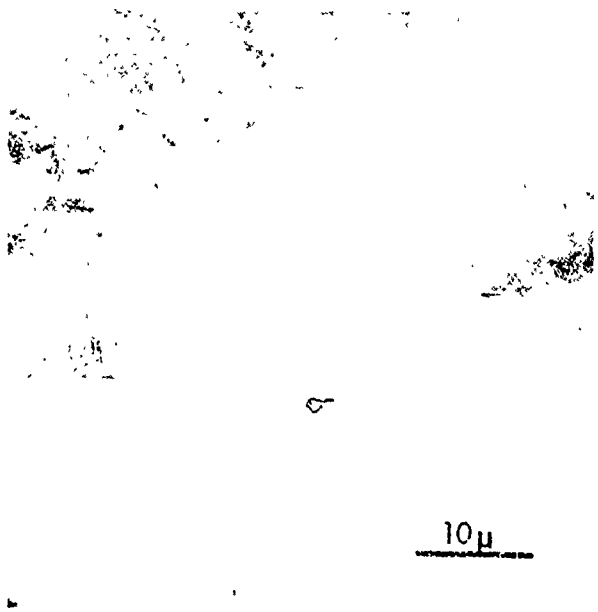

b

FIGURE 12 Bore Surface after Grit Blast Test at 0° Impingement Angle (SEM)

a

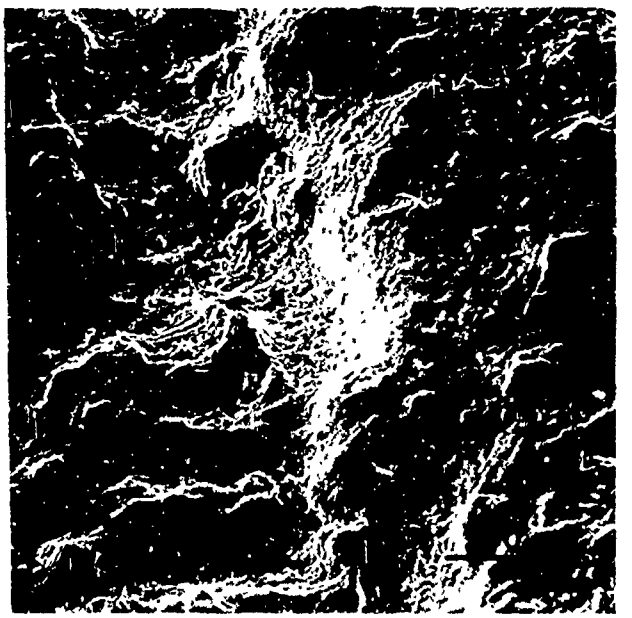

b

FIGURE 13 Bore Surface after Grit Blast Test at 90° Impingement Angle (SEM)

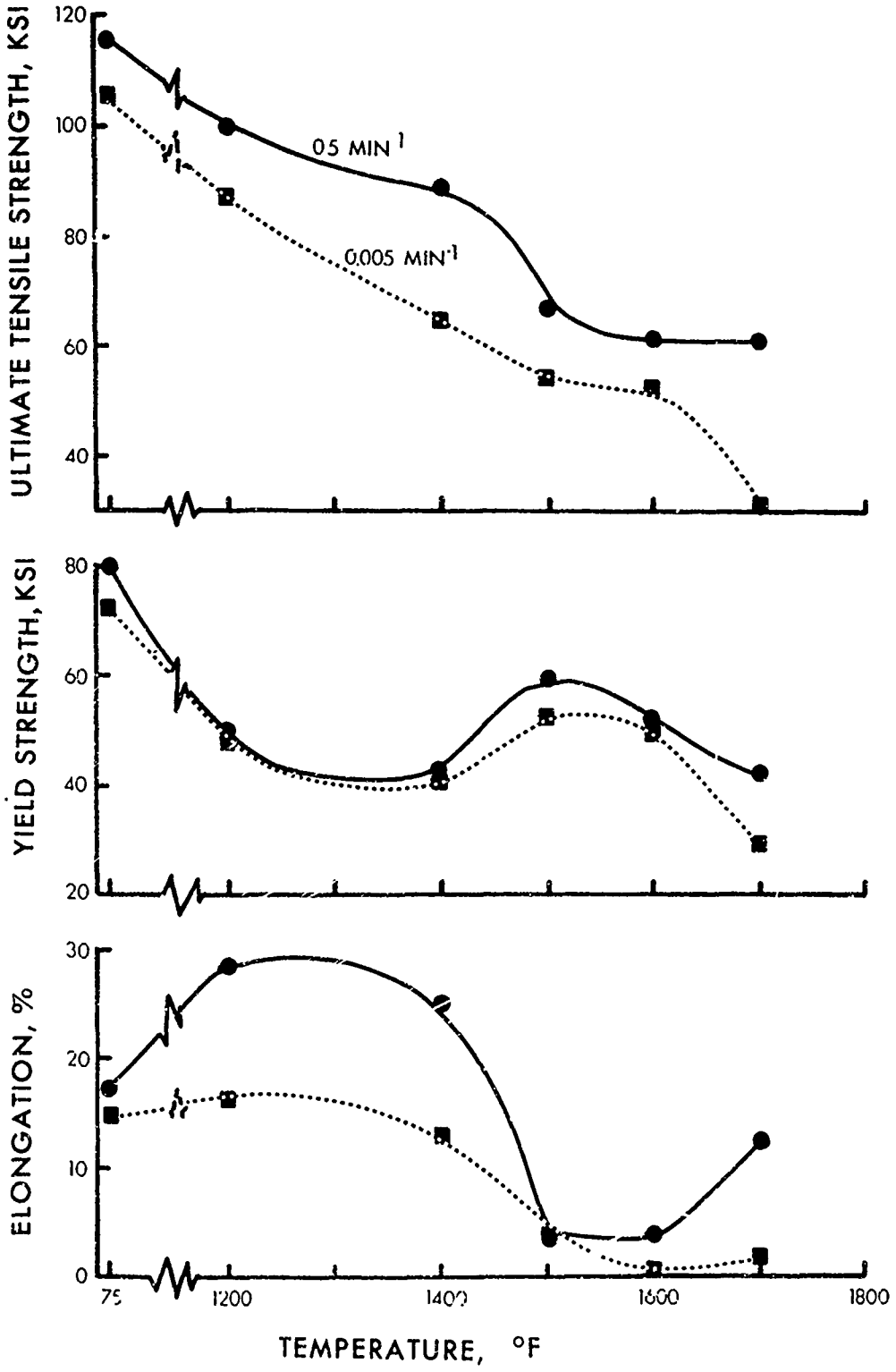

FIGURE 14 Elevated Tensile Properties of HS-21

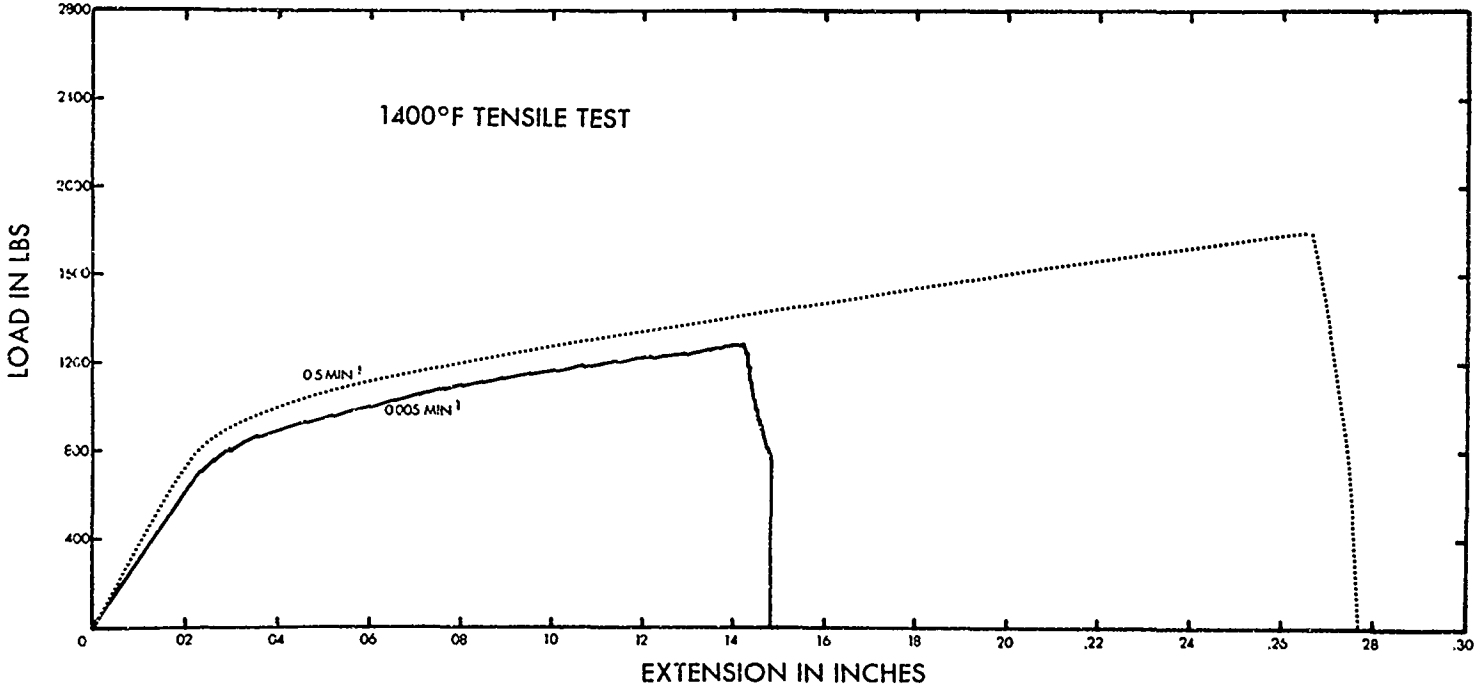

FIGURE 15 1400°F Tensile Test on Cast HS-21 at Two Different Strain Rates

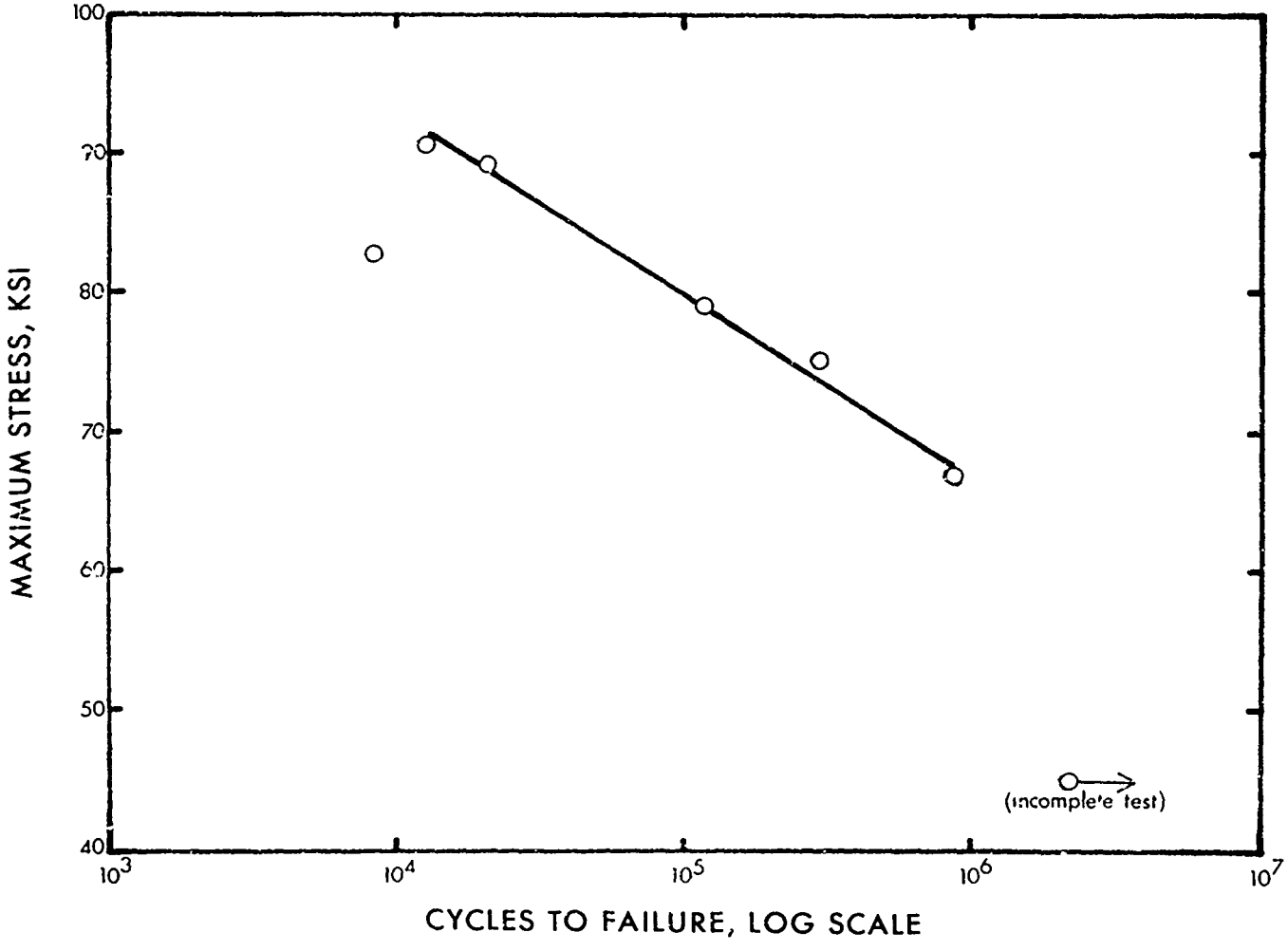

FIGURE 16 Room Temperature Fatigue Properties of HS-21

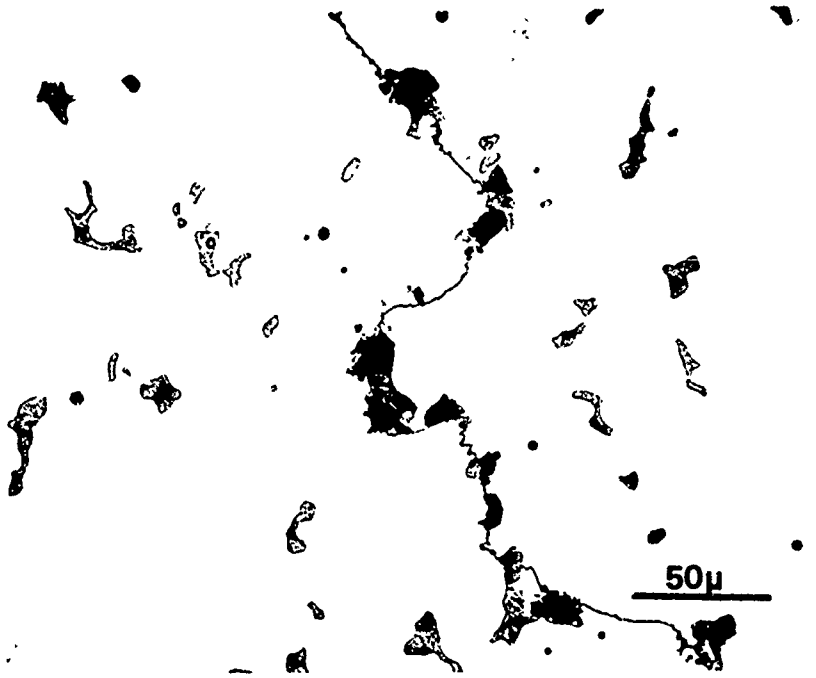

FIGURE 17 As-Cast Microstructure of HS-21

FIGURE 18 HS-21 Microstructure after 10 Minute Exposure at 2240°F

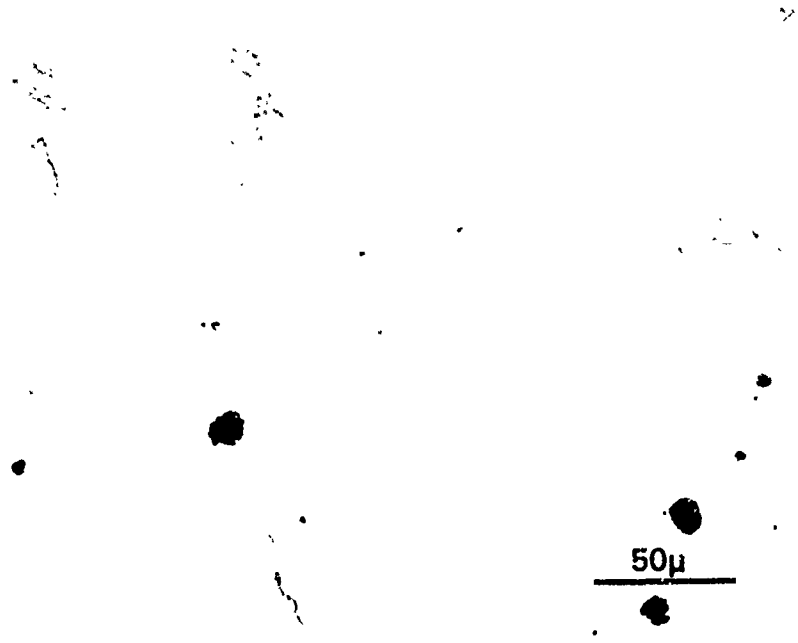

FIGURE 19 HS-21 Microstructure after 10 Minute Exposure at 2280°F

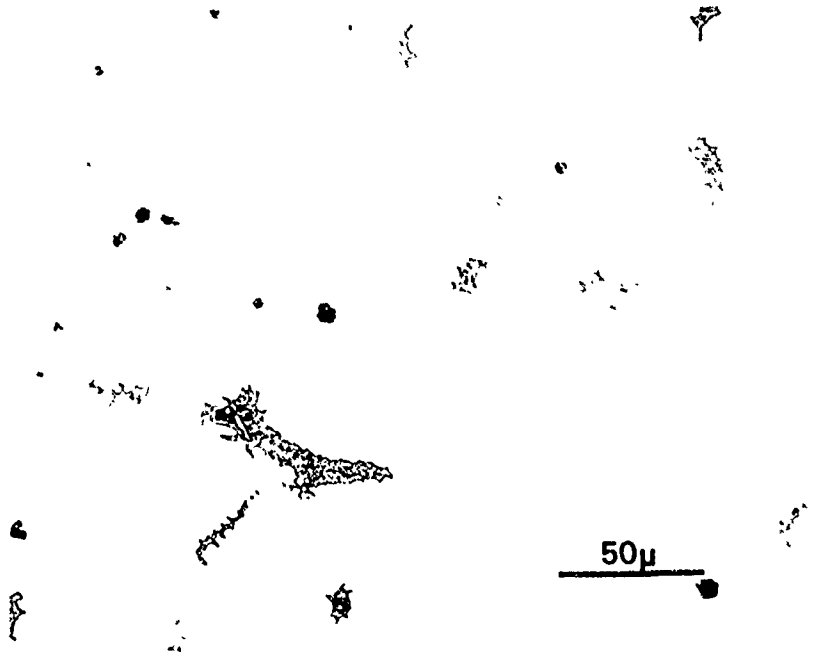

FIGURE 20 HS-21 Microstructure after 10 Minute Exposure at 2310°F

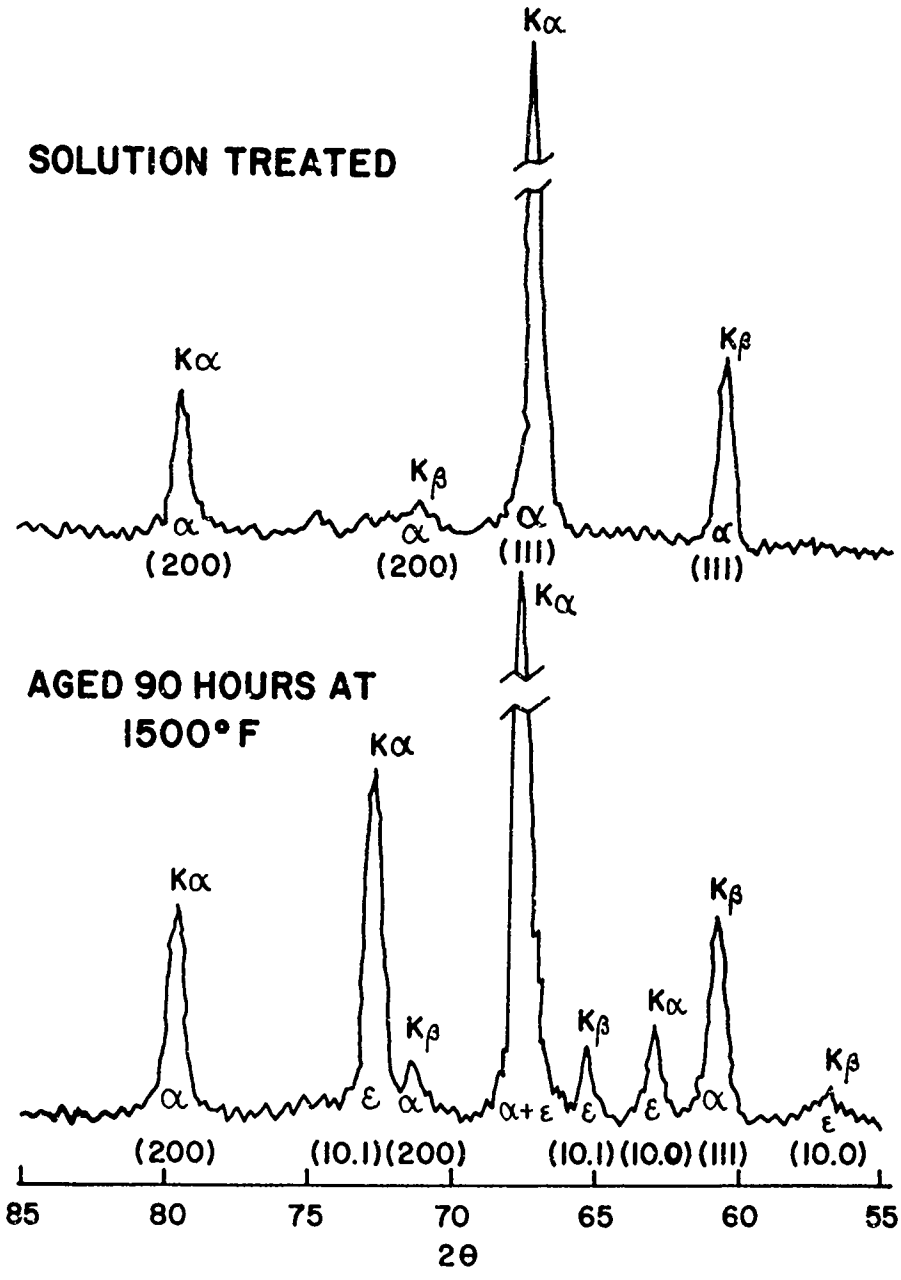

FIGURE 21 Change in X-Ray Diffraction Lines by 1500°F Aging Treatment on HS-21

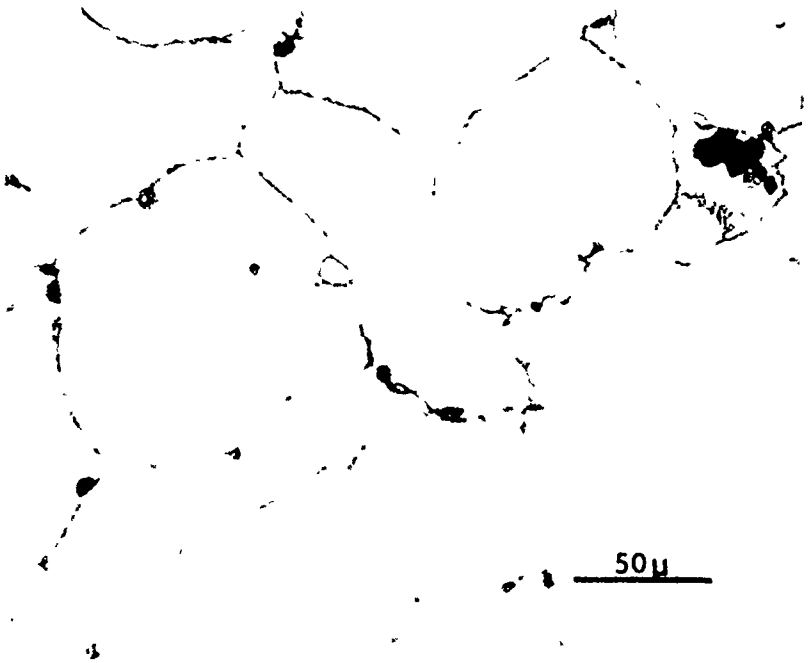

a. Solution-Annealed Structure

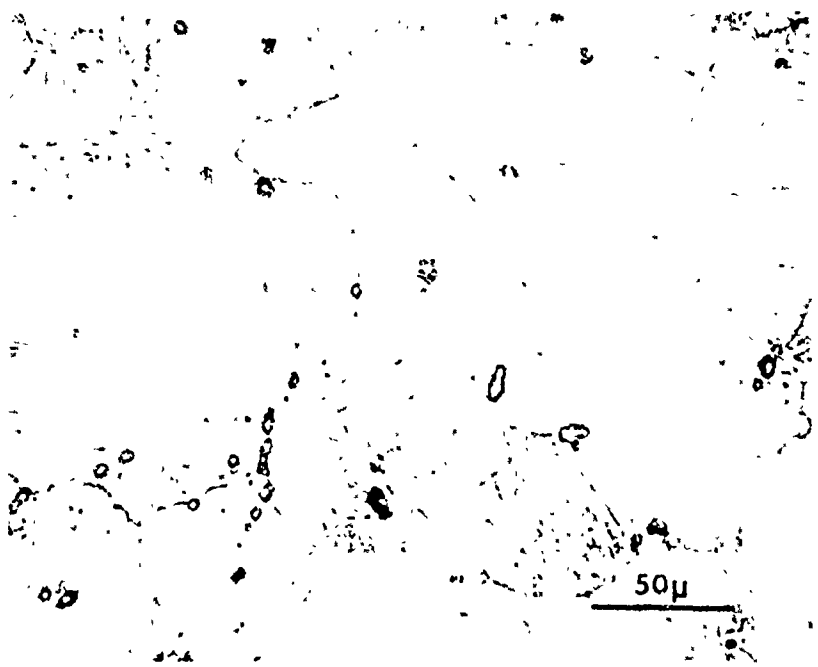

b. Aged Structure

FIGURE 22 Change in HS-21 Microstructure after 1500°F Aging Treatment

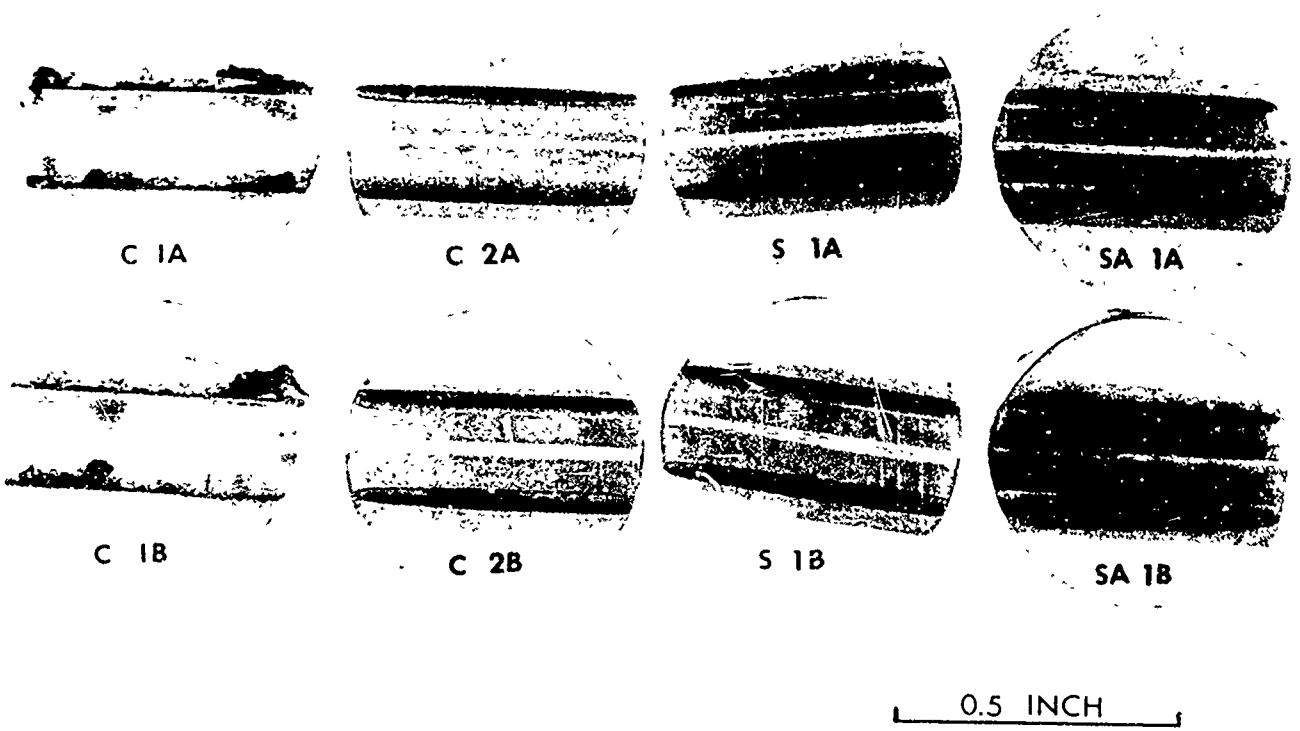

FIGURE 23 Falex Wear Test Specimens

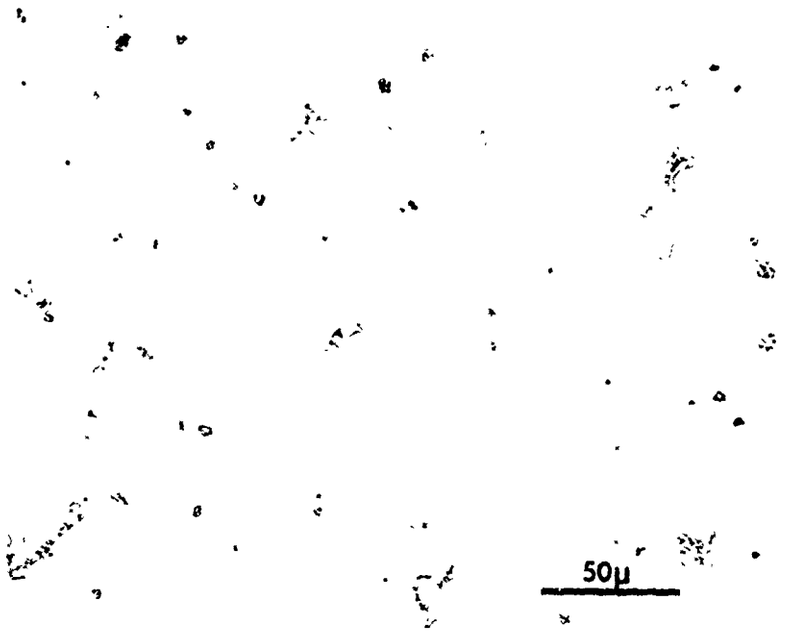

a. Heat Treated 2 Hrs at 2150°F

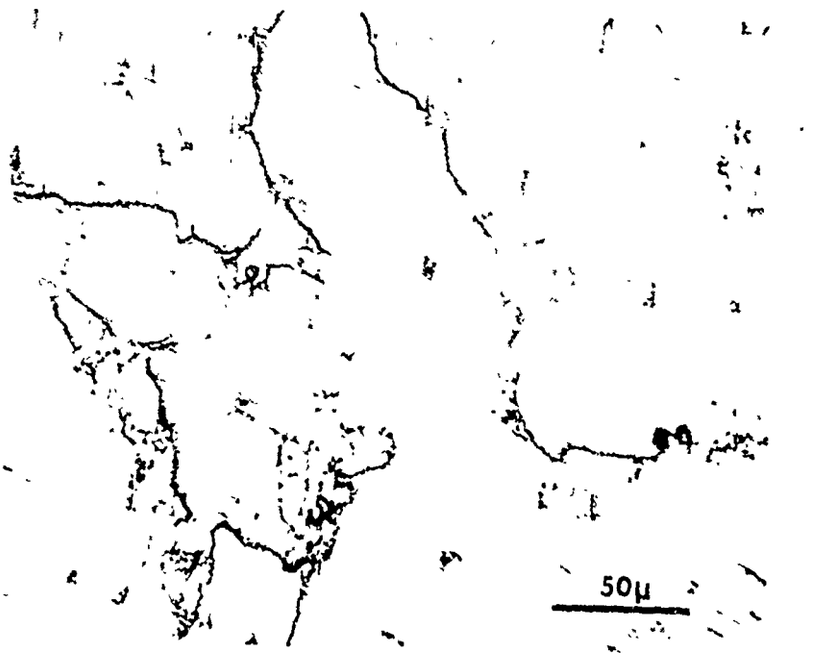

b. Heat Treated 2 Hrs at 2150°F + 50 Hrs at 1350°F

FIGURE 24 Microstructures of HS-21 Falex Wear Test Specimens

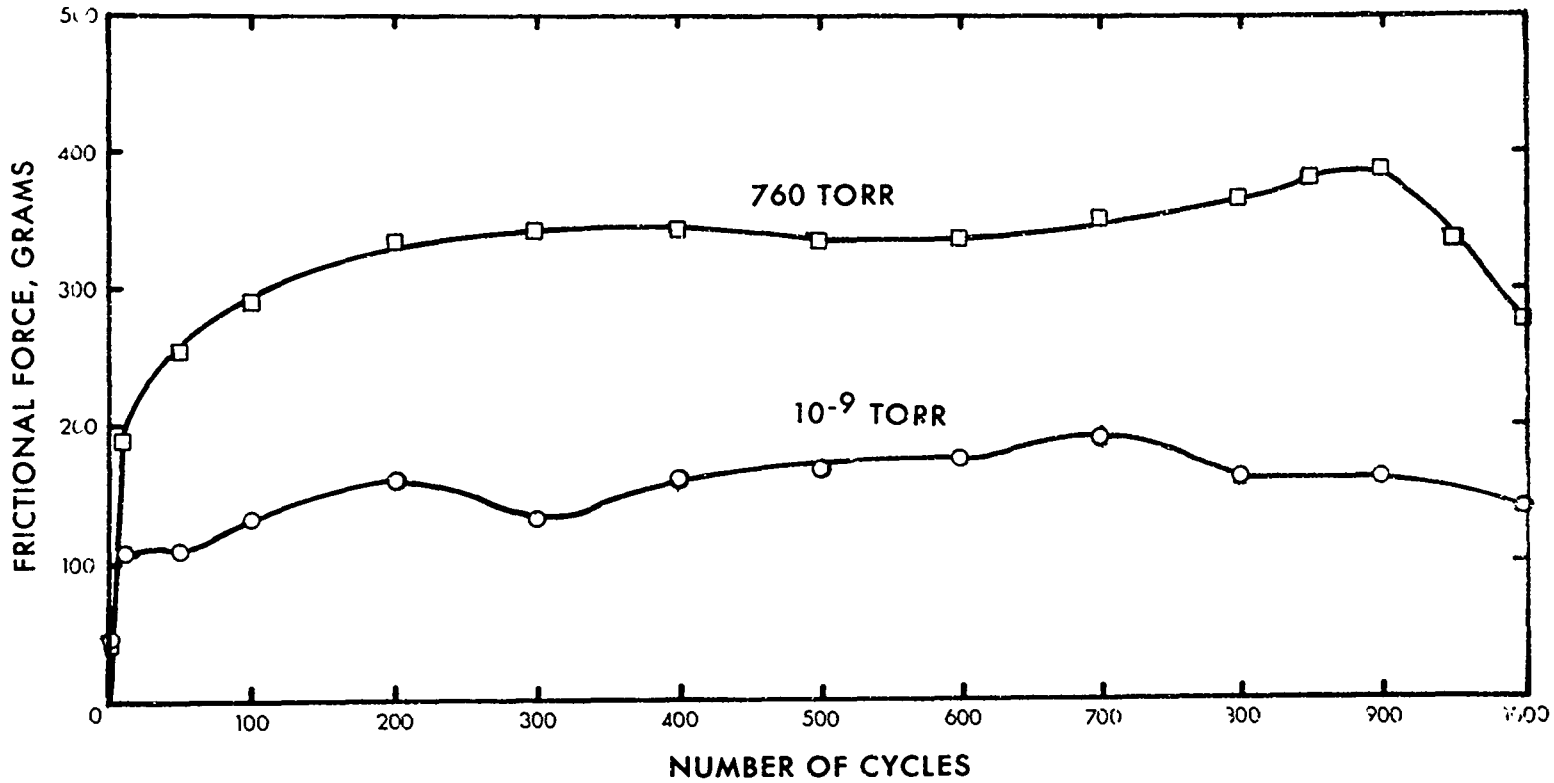

FIGURE 25 Frictional Force vs Number of Cycles Trace for HS-21 Specimens in Two Environments

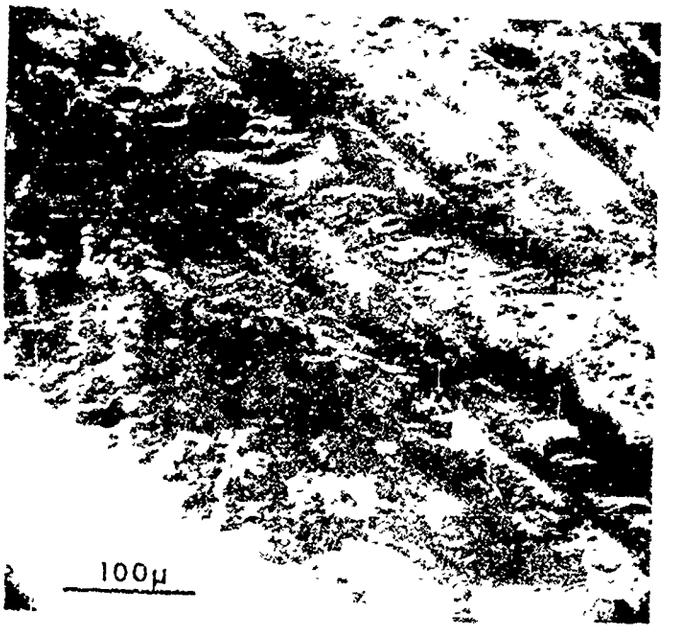

a. Secondary Electron Emission (S.E.) Mode

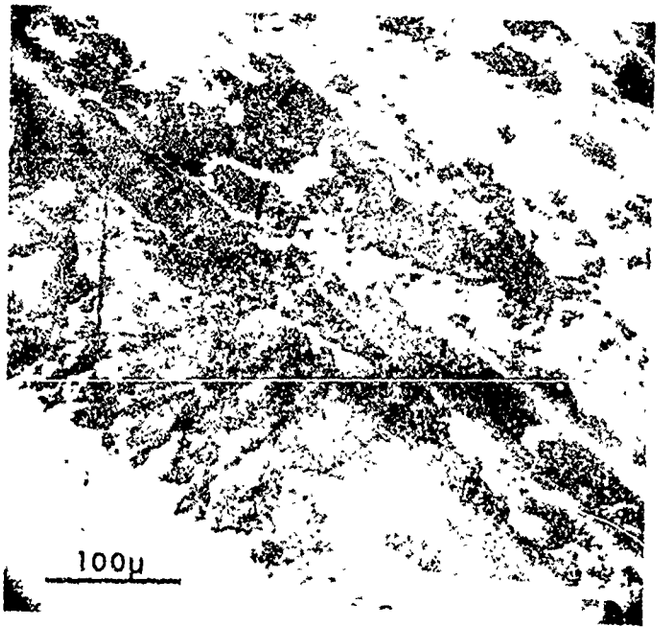

b. Back-Scatter Electron (B.E.) Mode

FIGURE 26 SEM Photographs of Wear Track on Specimen No. 7

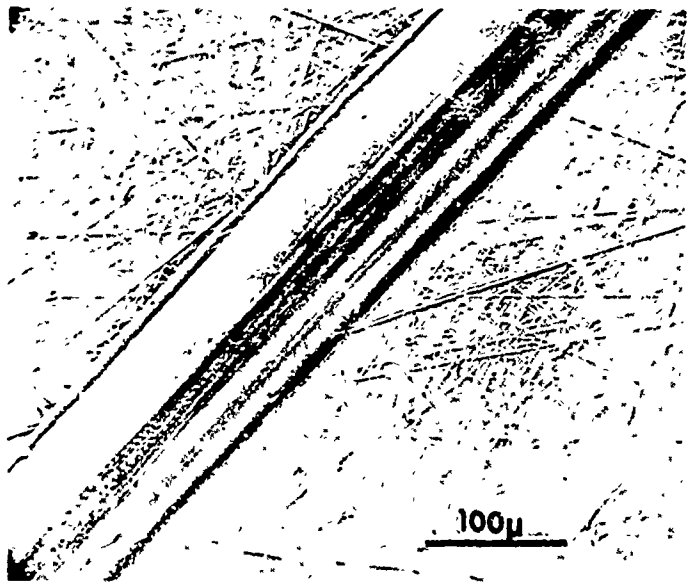

FIGURE 27 SEM Photograph of Wear Track (Test No. 8)

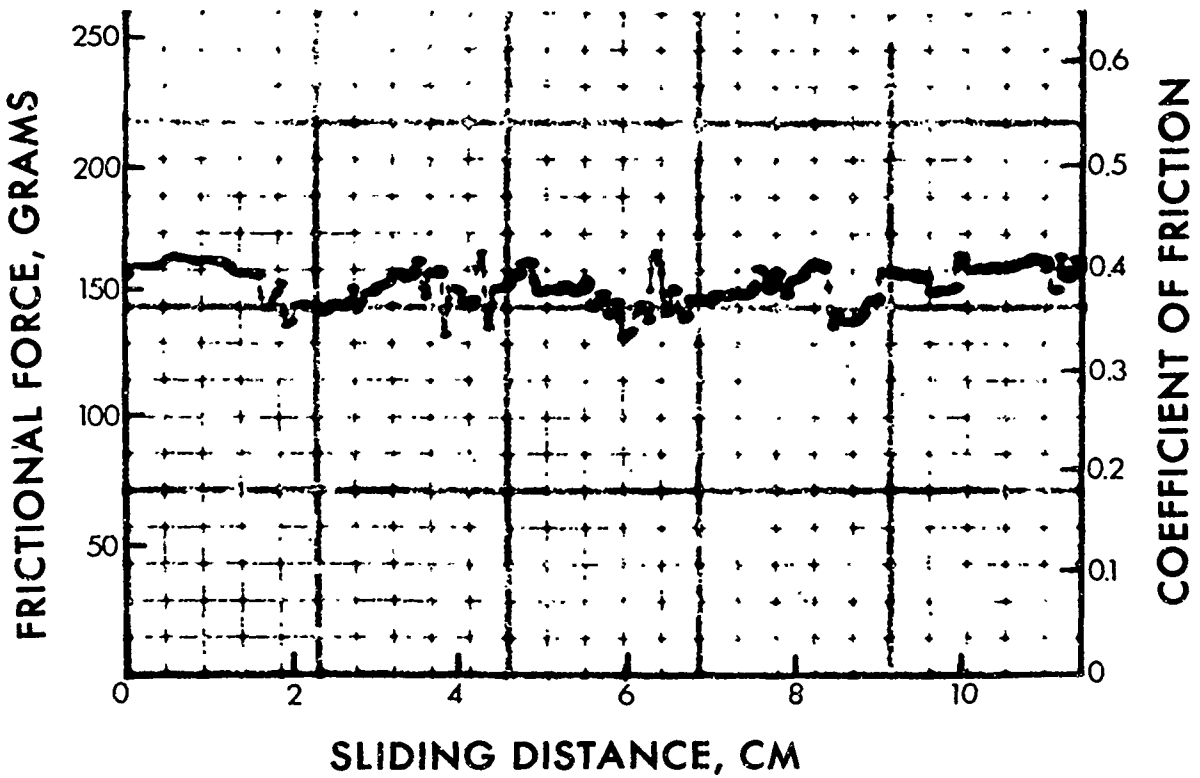

FIGURE 28 Typical Frictional Force - Distance Trace During One Pass

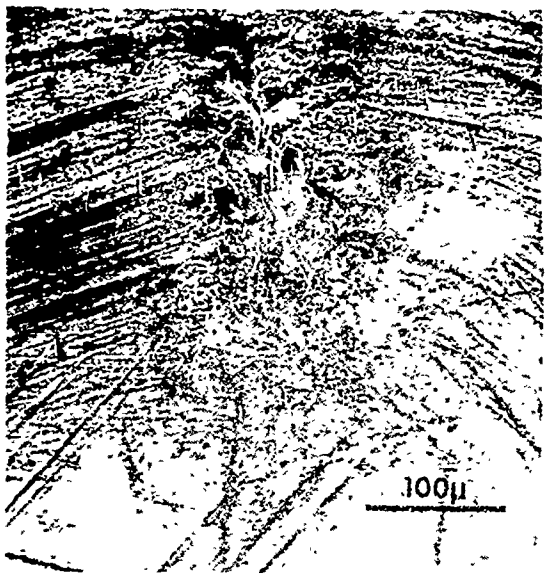

a. S.E. Mode

b. B.E. Mode

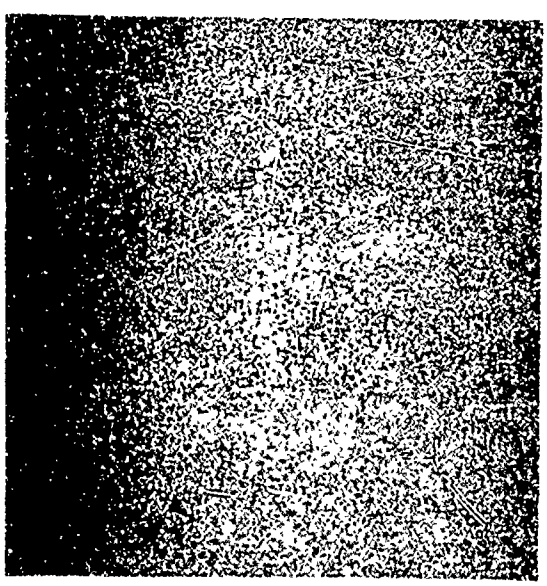

c. Cobalt Kα Image

d. Tungsten Lα Image

FIGURE 29 SEM Analysis of Residue on Stylus Surface

LITERATURE CITED

1. Badger, F. S., J. Metals, Vol. 10, p. 512, (1958).

2. Sullivan, C. P., Donachie, Jr., M. J., and Morral, F. P., Cobalt Monograph Series: Cobalt-base Superalloys, 1970, p. 1, Centre D'Information Du Cobalt, Brussels, (1970).

3. "Hypervelocity Guns and the Control of Gun Erosion," Summary Technical Report of Division 1, p. 331, NDRC, Vol. I, Washington, D. C., (1946).

4. "Investigation of Gun Erosion at the Geophysical Laboratory," Vol. III, January 1944 to July 1944, OSRD 4345, Report No. A-300, Geophysical Laboratory, CIW, (1944).

5. Osborn, E. F., "The Testing of Erosion-Resistant Materials and the Development of Improved Machine Gun Barrels," OSRD 6480, Report No. A-409, Geophysical Laboratory, CIW, (1945).

6. Cotterman, F. D., Siegler, W. A. and Magos, J. P., "Gun Barrel Liners - Materials, Insertion and Testing," OSRD 6479, Report No. A-408, Crane Company, (1946).

7. Ebihara, W. T., "Structural Stability of a Cast Co-Cr-Mo Alloy During Impulsive Thermal-Mechanical Loading," AD 721895, (1970)

8. Kotval, P. S., Trans, AIME, Vol. 242, p. 1951, (1968).

9. Private communication with Dr. D. H Buckley, NASA - Lewis Research Center, Dec. 1969.

10. Bitter, J. G. A., Wear, Vol 6, p. 5, (1963).

11. Finnie, I., Wear, Vol. 3, p. 87, (1960).

12. Neilson, J. H. and Gilchrist, A., Wear, Vol. 11, p. 111, (1968).

13. Union Carbide Corporation, Stellite Division (presently Cabot Corporation) Brochure Information, March, 1964.

14. Woodford, D. A. and McMahon, Jr., C. J., Second International Conference on the Strength of Metals and Alloys, p. 1067, American Society for Metals, Metals Park, Ohio, (1970).

APPENDIX

Nelson and Gilchrist[12] assumed that the following factors should be taken into account for any relationships describing erosion damage:

1. The normal component of kinetic energy of the impacting particles is absorbed in the specimen surface and accounts for deformation wear, which is associated with the repetitive blows encountered. These blows will eventually cause cracking and spalling of the surface material, and can be considered a fatigue phenomenon.

2. For certain hard materials, subjected primarily to deformation wear, a limiting component of velocity exists normal to the surface below which no erosion takes place.

3. The kinetic energy component parallel to the surface is associated with cutting wear.

4. For cutting wear and large angles of attack, the particles come to rest in the surface, and the total parallel component of kinetic energy contributes to cutting wear.

Therefore, if ϕ units of kinetic energy must be absorbed by the surface to release one unit mass of eroded material and, correspondingly, if ε energy units are necessary for deformation wear, then the following relationships exist:

$$W = \frac{\frac{1}{2}M(V^2 \cos^2\alpha - V_p}{\phi} + \frac{\frac{1}{2}M(V \sin \alpha - V_{el})^2}{\varepsilon} \quad \text{for } \alpha<\alpha_o$$

and

$$W = \frac{\frac{1}{2}MV^2 \cos^2\alpha}{\phi} + \frac{\frac{1}{2}M(V \sin \alpha - V_{el})^2}{\varepsilon} \quad \text{for } \alpha>\alpha_o$$

Where W = erosion produced

M = units of mass of particles impinging

α = angle of attack of impingment

V = particle velocity

V_{el} = critical velocity component normal to the surface below which no erosion takes place for certain hard materials

V_p = residual parallel component of particle velocity at small angles of attack

α_o = angle of attack at which V_p is zero

For particle velocities under 0.5 Mach, the values of both ϕ and ε depend on velocity and geometry of the erosive particles. At higher velocities, the hardness and shape of the abrasive become of minor importance as evidenced in liquid droplet erosion studies. The quantities ϕ and ε are difficult to define, although ϕ may be more apt to be related to mechanical properties such as hardness, yield or tensile strength whereas ε is more apt to be related to fatigue or fracture resistance properties.